Study of Airy Beams Generated via Four-Wave Mixing Process in a Homogeneous Atomic Medium

Li Li[1] Li Shuli[1] Zhang Yunzhe[1] Li Yuanyuan[1] Xu Kewei[1,2]
[1]*Institute of Applied Physics, Xi'an University of Arts and Science, Xi'an, Shaanxi 710065, China*
[2]*Nano-film and Biological Materials Research Center, Xi'an Jiaotong University, Xi'an, Shaanxi 710049, China*

Abstract Airy beams generated by the four-wave mixing (FWM) process in a homogeneous atomic medium is investigated. It is shown that Airy beams generated by both pure-FWM (PFWM) and dressed-FWM (DFWM) processes exhibit accelerating dynamics with a parabolic trajectory. The acceleration rate of these Airy beams can be dramatically modified by changing the detuning and strength of the external fields applied to the system. Due to nonlinear change of atomic coherence and the refractive index of resonant atoms induced by the dressing field, the amplitude suppression (enhancement) and the deflection position variation of DFWM signals can be achieved simply by changing the detuning of the dressing field. Airy beams generated via the FWM process can possibly be a powerful tool for delivering optical power, resonant particle manipulation and optical information processing.

Key words nonlinear optics; four-wave mixing; Airy beam; enhancement; suppression
OCIS codes 140.3295; 140.3300; 190.4380

均匀原子介质中四波混频产生艾里光束的研究

李 莉[1] 李姝丽[1] 张云哲[1] 李院院[1] 徐可为[1,2]
[1]西安文理学院应用物理研究所, 陕西 西安 710065
[2]西安交通大学纳米薄膜与生物材料研究中心, 陕西 西安 710049

摘要 研究了均匀原子介质中借助四波混频(FWM)产生的艾里光束。发现纯FWM(PFWM)及缀饰FWM(DFWM)过程产生的艾里光束均表现出抛物线路径加速的动力学特征,其加速率可通过调整作用于系统的外加光场的失谐量及强度得到显著改变。由于缀饰场的作用使得共振原子的原子相干及折射率产生非线性变化,DFWM信号的增强(抑制)及偏转位置的改变可简单通过调整缀饰场的失谐实现。这种FWM产生的艾里光束可望用于光能量传输、共振粒子操控及光信息处理。

关键词 非线性光束; 四波混频; 艾里光束; 增强; 抑制
中图分类号 O433 **文献标识码** A
doi: 10.3788/LOP52.081406

1 Introduction

Airy beam has attracted a lot of attention in recent years[1-12], because it has properties of resistance to diffraction, accelerating dynamics along the transverse direction during propagation, and self-healing when perturbations are imposed on them[1-4]. These exotic features of Airy beams may have many applications, e.g., controlling beam trajectory[5], particle manipulation[6], plasma channel generation[7] and near-field imaging of Airy surface plasmons[8].

In a previous discussion, Airy beams were generated by using linear diffractive elements only. However, a nonlinear process enables Airy beams to be at a new wavelength, and can be controlled by external fields, e.g., three-wave mixing and four-wave mixing (FWM) processes. A second-harmonic Airy beam and the

收稿日期: 2014-11-24; **收到修改稿日期**: 2015-04-13; **网络出版日期**: 2015-07-22
基金项目: 西安市科技计划项目(CX12189WL03)
作者简介: 李 莉(1972—),女,实验师,主要从事高分辨率光谱方面的研究。E-mail: lilinxcn@aliyun.com

tuning properties of the nonlinear interaction and propagation dynamics of the pump and second-harmonic output beams have been investigated by Arie A, et al. in asymmetric nonlinear photonic crystals[9-11]. Experimental generation of Airy beams has been achieved via the FWM process in hot rubidium vapor. After satisfying the phase matching condition, a FWM field with the profile of an Airy beam can be generated[12]. It was also shown that the acceleration rate, the intensities of the transmitted and selective reflected Airy beam can be modulated by external fields applied to the system[13-14]. Motivated by these works, we devote ourselves to the phenomena associated with the nonlinear generation of Airy beams by four-wave mixing (FWM) processes in our discussion. Without two-photon coherence, the efficiency of FWM is lower at resonance because the nonlinear optical processes are suppressed by the linear susceptibility[15]. However, by use of coherent population trapping[16] or electromagnetically induced transparency (EIT)[16-18] preparing for maximal atomic coherence, FWM processes can be dramatically enhanced since the weak generated signals can be allowed to transmit the resonant atomic medium with little absorption[19-22]. This control of FWM can be used in the application of the transfer of trans-spectral orbital angular momentum[23] and in optical images[24], and the generation of superluminal light pulses[25] and surface solitons[26].

2 Theoretical model

We consider the beam configuration shown in Fig.1(a). Beam 1 represents the probe field E_1. Beams 2 and 3 with a small angle (about $0.5°$) between them display the three fields E_2, E_3 and E_3', respectively. A reverse Y-type four-level system is shown in Fig.1(b), where $|0\rangle$ and $|3\rangle$ are two hyperfine levels of the ground state of the atom, and $|1\rangle$ and $|2\rangle$ are selected as the intermediate and the excited states, respectively. The transition frequencies of $|0\rangle-|1\rangle$, $|1\rangle-|2\rangle$ and $|3\rangle-|1\rangle$ are Ω_1, Ω_2 and Ω_3, respectively. We denote ω_i, $\Delta_i=\Omega_i-\omega_i$, $g_i(g_i')$ and $k_i(k_i')$ $(i=1,2,3)$ as the frequency, the detuning, the Rabi frequency and the wave vector of field $E_i\,(E_i')$, respectively. The decay rate from level $|i\rangle$ to $|j\rangle$ $(i,j=0,1,2,3,i\neq j)$ is defined as $\Gamma_{ij}=\Gamma_{ji}=(\Gamma_i+\Gamma_j)/2$ with $\Gamma_i(\Gamma_j)$ being the decay rates of level $|i\rangle$ ($|j\rangle$). When the phase-matching condition $\boldsymbol{k}_F=\boldsymbol{k}_1+\boldsymbol{k}_3-\boldsymbol{k}_3'$ is satisfied, a FWM signal propagating almost opposite to beam 3 is generated.

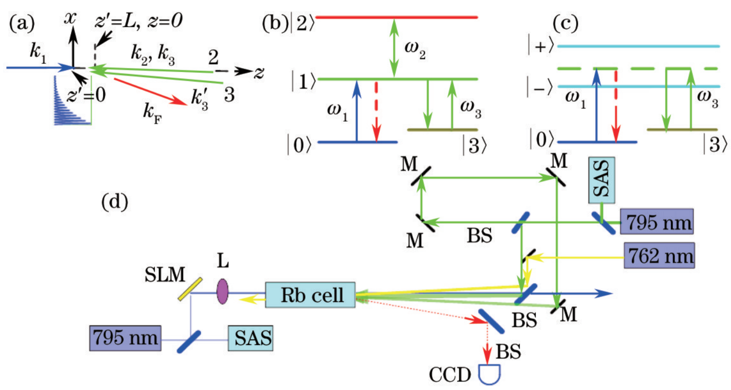

Fig.1 (a) Geometrical configuration of driving fields applied to the system; (b) reverted-Y-type four-level system; (c) dressed-state picture in (b); (d) possible experimental setup, with abbreviations: BS, beam splitter; SLM, spatial light modulator; L, lens; SAS, saturated absorption spectroscopy; CCD, charge-coupled device; and M, mirror

We assume that the probe field is a finite- power coupling Airy beam, whose transverse input amplitude at $z'=0$ can be expressed as

$$E_1(x,z'=0)=\pm A\mathrm{i}\left(\frac{x}{x_0}\right)\exp\left(\pm a\frac{x}{x_0}\right), \tag{1}$$

where a is the truncation factor and x_0 an arbitrary transverse scale, z' is the coordinate in the atomic sample.

Applying a Fourier transform (FT) to the probe field, we can decompose it into many plane wave components. The FWM coefficient of each component is denoted as $F(k)$. Taking the inverse FT, the probe wave $E_1(x,z')$ and the generated FWM wave $E_F(x,z)$ can be given by

$$E_1(x,z')=\frac{1}{2\pi}\int_{-\infty}^{\infty}E_1(k)\exp(\mathrm{i}kx+\mathrm{i}q_1z')\mathrm{d}k\ , \tag{2}$$

$$E_F(x,z)=\frac{1}{2\pi}\int_{-\infty}^{\infty}E_1(k)F(k)\exp(\mathrm{i}kx+\mathrm{i}q_Fz)\mathrm{d}k\ , \tag{3}$$

where $q_1=\sqrt{(k_1n)^2-k^2}$ and $q_F=\sqrt{(k_Fn)^2-k^2}$ are the Fourier component wave numbers of the probe and the generated FWM fields, respectively, with n being the refractive index of the atomic sample, z is the coordinate out of the atomic sample.

Each component of the nonlinear polarization responsible for the FWM signal is proportional to the third-order density matrix element $\sigma_{10}^{(3)}(k)$. To calculate $\sigma_{10}^{(3)}(k)$, we assume that E_1, E_3 and E_3' are weak fields, where as the dressing field E_2 can be of arbitrary magnitude. We also assume that the initial conditions for following coupling equations are $\sigma_{00}^{(0)}=1$ and $\sigma_{i0}(t=0)=0\ (i=1,2,3)$.

If the dressing field E_2 is applied to the transition $|1\rangle-|2\rangle$, the system can be treated as a dressed FWM (DFWM) process. In this situation, level $|1\rangle$ is dressed by E_2 to two split levels $|+\rangle$ and $|-\rangle$ [Fig.1(c)]. $\sigma_{10}^{(3)}(k)$ can be calculated by a process (I): $\sigma_{00}^{(0)}\xrightarrow{\omega_1}\sigma_{\pm0}^{(1)}\xrightarrow{\omega_3}\sigma_{30}^{(2)}\xrightarrow{-\omega_3}\sigma_{10}^{(3)}(k)$ together with the following coupling equations

$$\partial\sigma_{\pm0}^{(1)}/\partial t=-\Lambda_{10}\sigma_{\pm0}^{(1)}+\mathrm{i}g_1^{(k)}\sigma_{00}^{(0)}+\mathrm{i}g_2\sigma_{20}\ , \tag{4}$$

$$\partial\sigma_{20}/\partial t=-\Lambda_{20}\sigma_{20}+\mathrm{i}g_2\sigma_{\pm0}^{(1)}\ , \tag{5}$$

$$\partial\sigma_{30}^{(2)}/\partial t=-\Lambda_{30}\sigma_{30}^{(2)}+\mathrm{i}g_3\sigma_{\pm0}^{(1)}\ , \tag{6}$$

$$\partial\sigma_{10}^{(3)}(k)/\partial t=-\Lambda_{10}\sigma_{10}^{(3)}(k)+\mathrm{i}g_3'\sigma_{30}^{(2)}\ , \tag{7}$$

where the complex detunings Λ_{10}, Λ_{20} and Λ_{30} are respectively defined as $\Lambda_{10}=\Gamma_{10}+\mathrm{i}\Delta_1$, $\Lambda_{20}=\Gamma_{20}+\mathrm{i}(\Delta_1+\Delta_2)$ and $\Lambda_{30}=\Gamma_{30}+\mathrm{i}(\Delta_1-\Delta_3)$.Combining the perturbation chain (I) and the coupling equations (4)~(7), we then obtain the third-order solution

$$\sigma_{10}^{(3)}(k)=-\mathrm{i}g_1^{(k)}g_3g_3'\frac{\Lambda_{20}}{\Lambda_{10}\Lambda_{30}(\Lambda_{10}\Lambda_{20}+|g_2|^2)}\ . \tag{8}$$

When the dressing field E_2 is blocked, a pure FWM (PFWM) process for the Λ-type system $|0\rangle-|1\rangle$ $|3\rangle$ can be described by a perturbation chain (II): $\sigma_{00}^{(0)}\xrightarrow{\omega_1}\sigma_{10}^{(1)}\xrightarrow{\omega_3}\sigma_{30}^{(2)}\xrightarrow{-\omega_3}\sigma_{10}^{(3)}$, and the third-order solution for this case is

$$\sigma_{10}^{(3)}(k)=-\mathrm{i}g_1^{(k)}g_3g_3'/(\Lambda_{10}^2\Lambda_{30})\ . \tag{9}$$

Eq.(9) can be obtained from Eq.(8) by simply setting g_2=0.

By using the slowly varying amplitude approximation, the change rate of each generated FWM component along z can be derived from Maxwell's equations

$$\partial E_F(k)/\partial z'=\mathrm{i}2q_FN\mu_{10}\sigma_{10}^{(3)}(k)/\varepsilon_0\ , \tag{10}$$

where N is the number density of atoms, and μ_{10} is the transition dipole moment corresponding to $|0\rangle-|1\rangle$.

Combining Eqs.(8) and (10), we finally obtain

$$F(k)=C\Lambda_{20}/[\Lambda_{10}\Lambda_{30}(\Lambda_{10}\Lambda_{20}+|g_2|^2)]\ , \tag{11}$$

where $C=2q_FNL\mu_{10}^2g_3g_3'/(\varepsilon_0\hbar)$. For the PFWM process, Eq.(11) still holds.

Keeping the Taylor expansion of $q_F(k)=\sqrt{(k_Fn)^2-k^2}$ to the second order, i.e., $q_F(k)\approx k_Fn-k^2/(2k_1n)$, and substituting Eq.(11) into Eq.(3), the envelope function for the generated FWM beam can be expressed as

$$u(x,z)=\frac{1}{2\pi}\int_{-\infty}^{\infty}E_1(k)F(k)\exp\left[\mathrm{i}kx-\mathrm{i}\frac{(kk_1n)^2z}{2(k_Fn)^3}\right]\mathrm{d}k\,,\tag{12}$$

where the FT of the probe beam is given by $E_1(k)=x_0\exp[\mathrm{i}(\pm kx_0+\mathrm{i}a)^3/3]$.

3 Results and discussion

In numerical calculation, atomic parameters are chosen to correspond to the possible experimental setup shown in Fig.1(d) with the D_1 line of ^{85}Rb. The states of $|0\rangle$, $|1\rangle$, $|2\rangle$ and $|3\rangle$ correspond to levels $5S_{1/2}(F=2)$, $5P_{1/2}$, $5D_{1/2}$ and $5S_{1/2}(F=3)$, respectively. The decay rates are $\Gamma_0\approx\Gamma_3=2\pi\times0.01$ MHz, $\Gamma_1=2\pi\times5.75$ MHz and $\Gamma_2=2\pi\times0.8$ MHz. The wavelengths of E_1, E_3 (E_3') and E_2 are 794.799, 794.80 and 762 nm, respectively. For a cold atomic sample, we assume that L=2 mm, $N=6\times10^{15}$ cm^{-3}. The refractive index n can be calculated as $n=\mathrm{Re}[\sqrt{\varepsilon}]$, with $\varepsilon=1+\mathrm{i}3Nk_F^{-3}\Gamma_{10}\Lambda_{20}/(\Lambda_{10}\Lambda_{20}+g_2^2)$, where the strength of E_2 is assumed to be much larger than that of E_3 (E_3'). For a probe Airy beam, x_0=20 μm, a=0.1, and lobes develop toward negative x, i.e., $F_0(k')=x_0\exp[\mathrm{i}(k'x_0+\mathrm{i}a)^3/3]$.

In the following discussion, we assume that E_3 (E_3') and E_2 are set corresponding to the case of exact Raman detuning (i.e., $\Delta_3+\Delta_2=0$). In Figs.2 (a1), (a2), (a3) and (a4), we show the propagation of Airy beams generated by the PFWM (g_2=0) process for $\Delta_1=0,\ 10\Gamma_{10},\ 20\Gamma_{10}$ and $30\Gamma_{10}$, respectively, while in Figs.3 (a1), (a2), (a3) and (a4), we show the propagation generated by the DFWM (Δ_1=0) process for $g_2=0.6\Gamma_{10},\ \Gamma_{10},\ 2\Gamma_{10}$ and $5\Gamma_{10}$, respectively, where we assume that E_3 (E_3') and E_2 are exactly detuned to the transitions $|3\rangle-|1\rangle$ and $|1\rangle-|2\rangle$, respectively, i.e., $\Delta_3=\Delta_2=0$. The intensity profiles corresponding to Figs.2 (Figs.3) (a1), (a2), (a3) and (a4) are plotted in Figs.2 (Figs.3) (b1), (b2), (b3) and (b4), respectively, at various distances. Here, the amplitude is normalized with respect to the maximum value of the first lobe at the output position z=0.

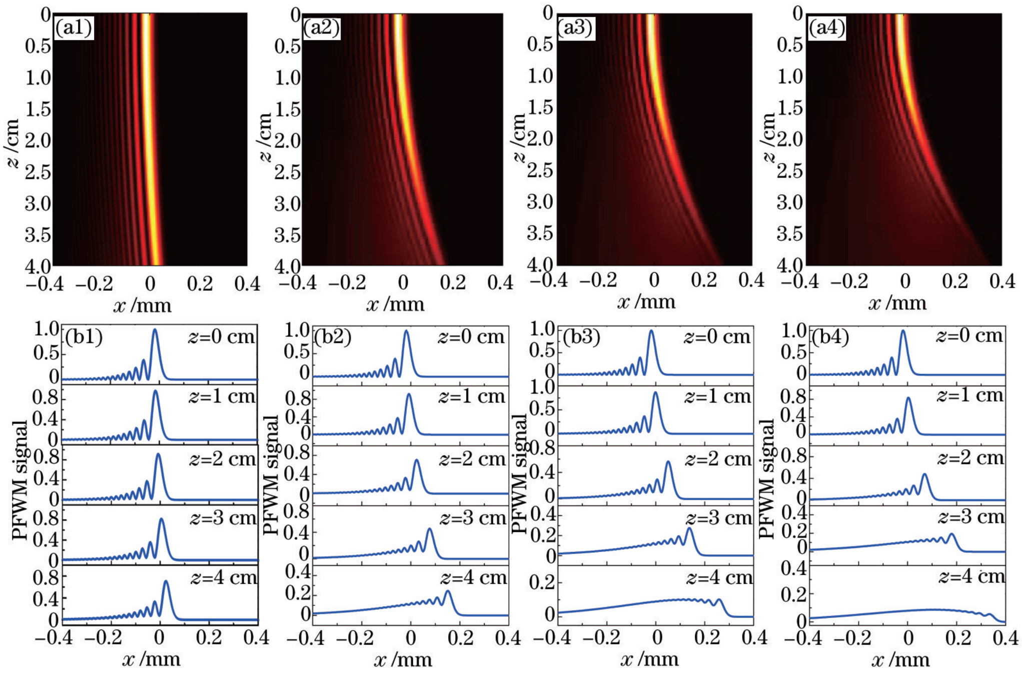

Fig.2 (a1)~(a4): Intensities of Airy beams generated by PFWM process. (b1)~(b4): Intensities versus x at different propagation distances, which correspond to (a1)~(a4) respectively. From (a1) [(b1)] to (a4) [(b4)], Δ_1=0, $10\Gamma_{10}$, $20\Gamma_{10}$ and $30\Gamma_{10}$, respectively

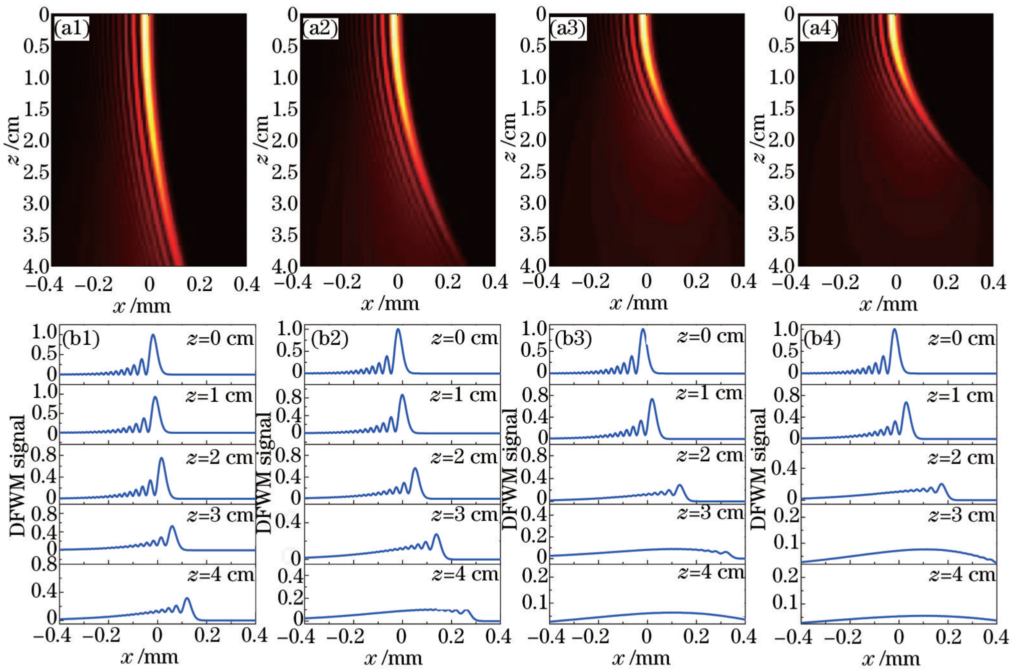

Fig.3 Figure setup is as Fig.2, but for Airy beams generated by DFWM process. From (a1) [(b1)] to (a4) [(b4)], $g_2 = 0.6\Gamma_{10}$, Γ_{10}, $2\Gamma_{10}$ and $5\Gamma_{10}$, respectively

It can be found that both PFWM and DFWM beams are quasi-diffraction-free Airy-like beams, that exhibit accelerating dynamics toward the same direction. The FWHM of the first lobe for PFWM and DFWM is ~36 μm. For the former case this width can remain almost invariant up to ~4, ~3.2, ~2.8 and ~2.5 cm for $\Delta_1 = 0$, $10\Gamma_{10}$, $20\Gamma_{10}$ and $30\Gamma_{10}$, respectively, while for the latter case, this width can remain up to ~3.7, ~2.8, ~1.8 and ~1.5 cm for $g_2 = 0.6\Gamma_{10}$, Γ_{10}, $2\Gamma_{10}$ and $5\Gamma_{10}$, respectively. Due to atom-field interaction, the quasi-diffraction-free character of the FWM beams can be dramatically modified by external fields applied to the system, the larger the probe detuning, the greater the acceleration rate of the PFWM beam; When all the fields are exactly tuned, i.e., double EIT conditions for two sub-systems $|0\rangle-|1\rangle-|2\rangle$ and $|3\rangle-|1\rangle-|2\rangle$ are satisfied, the acceleration rate of the DFWM beam can be largely modified by the strength of the dressing field, the larger the strength of the dressing field, the greater the acceleration rate of the DFWM beam. This modification is mainly due to the nonlinear change of atomic coherence and the refractive index of atomic medium induced by the dressing field.

We also show that the amplitude of DFWM signals can be largely suppressed or enhanced, see Fig.4 (a), where the amplitude is normalized by the maximum value of the first lobe in the PFWM process for $\Delta_1 = 0$. The suppression and enhancement of DFWM can be demonstrated by simple dressed state analysis, where the DFWM signal can be treated as a superposition of two FWM processes induced by the two subsystems $|0\rangle-|+\rangle-|3\rangle$ and $|0\rangle-|-\rangle-|3\rangle$, respectively. When the interaction of two FWM processes is a destructive interference (e.g., $\Delta_2 = -5\Gamma_{10}, 4.5\Gamma_{10}$), the DFWM signal is suppressed, while in the constructive case (e.g., $\Delta_2 = 5\Gamma_{10}$), the signal can be dramatically enhanced. The deflection position of DFWM signals is plotted in Fig. 4(b). In all three cases, there exists a maximum deflection for $\Delta_2 = -5\Gamma_{10}$ and a minimum deflection for $\Delta_2 = 4.5\Gamma_{10}$ respectively. This deflection is due to the change of refractive index modified by the dressing field. It is apparent that the lateral position of the DFWM beam can be simply controlled by changing the detuning of the dressing field. This tunable optical behavior may have some potential applications in medicine science[13].

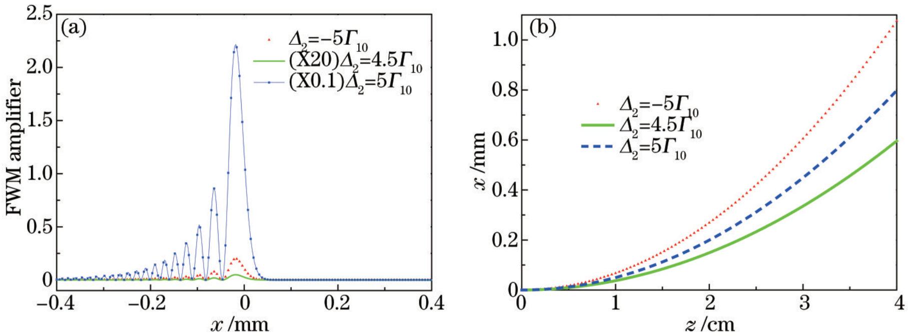

Fig.4 (a) Normalized amplitude; (b) lateral position of DFWM signals. Triangles (red), solid (green) lines, and short dashed (blue) lines for $\Delta_2 = -5\Gamma_{10}$, $4.5\Gamma_{10}$ and $5\Gamma_{10}$, respectively. Other parameters are $\Delta_1 = -5\Gamma_{10}$ and $g_2 = 5\Gamma_{10}$

4 Conclusion

We have examined Airy beams generated by the FWM process in a homogeneous atomic medium. It is shown that both PFWM and DFWM beams are quasi-diffraction-free Airy-like beams, that exhibit accelerating dynamics toward the same direction. The acceleration rates of these Airy beams can be dramatically modified by the external fields applied to the system. We also show that the amplitude suppression (enhancement) and the deflection position of the generated DFWM signals can be modified simply by changing the detuning of the dressing field. This modification is due to the nonlinear change of atomic coherence and the refractive index induced by the dressing field. Airy beams generated via FWM processes can possibly be a powerful tool in the use of optical power delivering, resonant particle manipulation and optical information processing.

References

1 Siviloglou G, Christodoulides D. Accelerating finite energy Airy beams[J]. Opt Lett, 2007, 32(8): 979-981.

2 Siviloglou G, Broky J, Dogariu A, *et al.*. Observation of accelerating Airy beams[J]. Phys Rev Lett, 2007, 99(21): 213901.

3 Broky J, Siviloglou G, Dogariu A, *et al.*. Self-healing properties of optical Airy beams[J]. Opt Express, 2008, 16(17): 12880-12891.

4 Chu X. Evolution of an Airy beam in turbulence[J]. Opt Lett, 2011, 36(14): 2701-2703.

5 Hu Y, Zhang P, Lou C, *et al.*. Optimal control of the ballistic motion of Airy beams[J]. Opt Lett, 2010, 35(13): 2260-2262.

6 Zhang P, Prakash J, Zhang Z, *et al.*. Trapping and guiding microparticles with morphing autofocusing Airy beams[J]. Opt Lett, 2011, 36(15): 2883-2885.

7 Polynkin P, Kolesik M, Moloney J, *et al.*. Curved plasma channel generation using ultraintense Airy beams[J]. Science, 2009, 324(5924): 229-232.

8 Minovich A, Klein A, Janunts N, *et al.*. Generation and near-field imaging of Airy surface plasmons[J]. Phys Rev Lett, 2011, 107(1): 116802.

9 Ellenbogen T, Voloch-Bloch N, Ganany-Padowicz A, *et al.*. Nonlinear generation and manipulation of Airy beams[J]. Nature Photonics, 2009, 3(7): 395-398.

10 Dolev I, Ellenbogen T, Arie A. Switching the acceleration direction of Airy beams by a nonlinear optical process[J]. Opt Lett, 2010, 35(10): 1581-1583.

11 Dolev I, Arie A. Three wave mixing of airy beams in a quadratic nonlinear photonic crystals[J]. Appl Phys Lett, 2010, 97(17): 171102.

12 Wei D, Yu Y, Cao M, *et al.*. Generation of Airy beams by four-wave mixing in Rubidium vapor cell[J]. Opt Lett, 2014, 39(15): 4557-4560.

13 Zhuang F, Shen J, Du X, *et al.*. Propagation and modulation of Airy beams through a four-level electromagnetic induced transparency atomic vapor[J]. Opt Lett, 2012, 37(15): 3054-3056.

14 Li Y, Li L, Lu Y, *et al.*. Selective reflection of Airy beam at an interface between dielectric and homogeneous atomic medium[J]. Opt Express, 2013, 21(7): 8311-8318.

15 Gea-Banacloche J, Li Y, Jin S, *et al.*. Electromagnetically induced transparency in ladder-type inhomogeneously broadened media: Theory and experiment[J]. Phys Rev A, 1995, 51(1): 576-584.

16 Scully M, Zubairy M. Quantum Optics[M]. Cambridge: Cambridge University, 1997.

17 Harris S. Electromagnetically induced transparency[J]. Phys Today, 1997, 50(7): 36-42.

18 Fleischhauer M, Imamoglu A, Marangos J. Electromagnetically induced transparency: optics in coherent media[J]. Rev Mod Phys, 2005, 77(2): 633-673.

19 Deng L, Payne M. Three-photon destructive interference in ultraslow-propagation-enhanced four-wave mixing[J]. Phys Rev A, 2003, 68(5): 051801.

20 Wu Y, Saldana J, Zhu Y. Large enhancement of four-wave mixing via EIT induced suppression of nonlinear photon absorptions[J]. Phys Rev A, 2003, 67(1): 013811.

21 Sun J, Zuo Z, Mi X, *et al.*. Two-photon resonant four-wave mixing in a dressed atomic system[J]. Phys Rev A, 2004, 70(5): 053820.

22 Zhang Y, Brown A, Xiao M. Opening four-wave mixing and six-wave mixing channels via dual electromagnetically induced transparency windows[J]. Phys Rev Lett, 2007, 99(12): 123603.

23 Walker G, Arnold A, Franke-Arnold S. Trans-spectral orbital angular momentum transfer via four-wave mixing in Rb vapor[J]. Phys Rev Lett, 2012, 108(24): 243601.

24 Ding D, Zhou Z, Shi B, *et al.*. Image transfer through two sequential four-wave mixing in a hot atomic vapor[J]. Phys Rev A, 2012, 85(5): 053815.

25 Glasser R, Vogl U, Lett P. Stimulated generation of superluminal light pulses via four-wave mixing[J]. Phys Rev Lett, 2012, 108(17): 173902.

26 Zhang Y, Yuan C, Zhang Y, *et al.*. Surface solitons of four-wave mixing in electromagnetically induced lattice[J]. Laser Phys Lett, 2013, 10(5): 055406.

栏目编辑：刘丰瑞